Folding of Insulin Receptor Monomers Is Facilitated by the Molecular Chaperones Calnexin and Calreticulin and Impaired by Rapid Dimerization

Joseph Bass,*‡ Gavin Chiu,§ Yair Argon,‖¶ and Donald F. Steiner‡§

*The Department of Medicine, ‡The Howard Hughes Medical Institute, §The Department of Biochemistry and Molecular Biology, ‖The Committee on Immunology, and ¶The Department of Pathology, The University of Chicago, Chicago, Illinois 60637

Abstract. Many complex membrane proteins undergo subunit folding and assembly in the ER before transport to the cell surface. Receptors for insulin and insulin-like growth factor I, both integral membrane proteins and members of the family of receptor tyrosine kinases (RTKs), are unusual in that they require homodimerization before export from the ER. To better understand chaperone mechanisms in endogenous membrane protein assembly in living cells, we have examined the folding, assembly, and transport of the human insulin receptor (HIR), a dimeric RTK. Using pulse-chase labeling and nonreducing SDS-PAGE analysis, we have explored the molecular basis of several sequential maturation steps during receptor biosynthesis. Under normal growth conditions, newly synthesized receptor monomers undergo disulfide bond formation while associated with the homologous chaperones calnexin (Cnx) and calreticulin (Crt). An inhibitor of glucose trimming, castanospermine (CST), abolished binding to Cnx/Crt but also unexpectedly accelerated receptor homodimerization resulting in misfolded oligomeric proreceptors whose processing was delayed and cell surface expression was also decreased by ~30%. Prematurely-dimerized receptors were retained in the ER and more avidly associated with the heat shock protein of 70 kD homologue binding protein. In CST-treated cells, receptor misfolding followed disordered oligomerization. Together, these studies demonstrate a chaperone function for Cnx/Crt in HIR folding in vivo and also provide evidence that folding efficiency and homodimerization are counterbalanced.

THE efficient production of membrane proteins is an essential function of the eukaryotic secretory pathway. One puzzling feature of the folding and assembly of nascent proteins studied to date is the great diversity in their rates of assembly and transport (Lodish and Kong, 1984; Helenius, 1994). Various studies indicate that a major rate-limiting event in the delivery of proteins to the distal secretory pathway is the time required for conformational maturation in the ER (Lodish, 1986; Aridor and Balch, 1996).

In the ER, the high concentration of nascent hydrophobic proteins, combined with the oxidative environment, increases the potential for aggregation and misfolding compared with conditions in the cytosol (Gething and Sambrook, 1992; Helenius et al., 1992; Hartl, 1996). Ultimately, a complex quality control network distinguishes functional oligomeric proteins from their misfolded counterparts. In both mammalian cells and in yeast, two major classes of ER chaperones are central components of the quality control network: these are (*a*) the heat shock protein of 70 kD (Hsp70)[1] homologue binding protein (BiP) (Munro and Pelham, 1986), and (*b*) the calcium-binding proteins calnexin (Cnx) and calreticulin (Crt) (Ou et al., 1993; Bergeron et al., 1994; Krause and Michalak, 1997).

The most detailed understanding of chaperone action in the ER has emerged from studies of the immunoglobulin heavy chain BiP. BiP participates in multiple steps during protein maturation, including translocation, formation of tertiary structure, and retrieval of misfolded proteins from the *cis*-Golgi (Munro and Pelham, 1986; Kozutsumi et al., 1988; Gething and Sambrook, 1992; Hammond and Hele-

Address all correspondence to Joe Bass, The University of Chicago, Howard Hughes Medical Institute, 5841 South Maryland Ave., MC 1028, Chicago, IL 60637. Tel.: (773) 702-1328. Fax: (773) 702-4292. E-mail: jbass@midway.uchicago.edu

1. *Abbreviations used in this paper*: BFA, brefeldin A; BiP, binding protein; Cnx, calnexin; Crt, calreticulin; CST, castanospermine; DSP, dithio*bis* (succinimidyl propionate); ECL, enhanced chemiluminescence; endo H, endoglycosidase H; HA, hemagglutinin; HIR, human insulin receptor; Hsp70, heat shock protein of 70 kD; PMSF, phenylmethlsulfonyl fluoride.

nius, 1994*a*,*b*; Brodsky et al., 1995; Lyman and Schekman, 1997).

Cnx and Crt have more recently emerged as ER resident chaperones that interact with newly synthesized glycoproteins in early stages of maturation (David et al., 1993; Ou et al., 1993; Hammond and Helenius, 1994*a*,*b*; Hammond et al., 1994; Jackson et al., 1994; Pind et al., 1994; Hebert et al., 1996). Mutant- or incompletely assembled subunits remain associated with calnexin for a prolonged period and are retained in the ER before degradation (Loo and Clarke, 1994). The basis for calnexin association with nascent proteins has been extensively investigated both in vivo with histocompatibility complexes and in vitro with viral hemagglutinin (HA) and vesicular stomatitis virus glycoprotein (Hebert et al., 1996; Vassilakos et al., 1996). An unusual feature of calnexin–substrate interactions that has emerged from these studies is that calnexin binds preferentially to N-linked oligosaccharides independent of substrate conformation (Zapun et al., 1997). Moreover, by using a specific inhibitor of glucosidases I and II in microsomes, Hebert and co-workers (1995) have presented evidence that substrate interactions are restricted to glycoproteins containing a single terminal glucose residue at N-linked sites, and that the subsequent effects on substrate folding are facilitated through this interaction. Accumulating evidence suggests that analogous effects mediate in vivo interactions between major histocompatability complex (MHC) class I and Cnx (Vassilakos et al., 1996). These observations, in combination with the observed decrease in formation of correctly folded HA trimers and MHC class I molecules in the presence of castanospermine (CST), a glucosidase inhibitor, suggest that Cnx acts as a chaperone in vivo. Nonetheless, it remains unclear whether a general chaperone function for Cnx/Crt in endogenous oligomeric protein folding exists and whether Cnx and/or Crt participate in quality control for such proteins.

Here we have analyzed the integrated effects of Cnx, Crt, and BiP on the folding, assembly, and trafficking of the insulin receptor, an endogenous membrane protein, in living cells. Initially, we followed the folding and trafficking of human insulin receptor (HIR) in pulse-chase experiments in heterologous cells expressing wild-type and uncleaved mutant HIR (R732A). We examined the role of disulfide bond formation in receptor maturation and found it to correspond with maximal binding of HIR monomers to Cnx/Crt in a glycan-dependent interaction. Disrupting maturation of N-linked glycans with CST, which was previously shown to reduce cell surface expression of HIR, blocked Cnx/Crt binding, accelerated dimerization, and resulted in ER retention (Arakaki et al., 1987). Together, our results indicate that the timing of HIR assembly is pivotal in ensuring high efficiency folding and that ER chaperones participate in HIR maturation by promoting folding before assembly.

Materials and Methods

Miscellaneous

Restriction enzymes and other reagents were purchased from Amersham Pharmacia Biotech., Inc. (enhanced chemiluminescence [ECL], Amplify; Piscataway, NJ), Epicentre Technologies Corp. (brefeldin A [BFA]; Madison, WI), Perkin-Elmer Corp. (Foster City, CA), New England Biolabs Inc. (Beverly, MA), Boehringer Mannheim Biochemicals (endoglycosidase H [endo H], neuraminidase, and protease inhibitors; Indianapolis, IN), Pierce Chemical Co. (cross-linkers; Rockford, IL), Wako Bioproducts (digitonin; Richmond, VA), Bio-Rad Laboratories (Hercules, CA), and Sigma Chemical Co. (CST; St. Louis, MO). mAb 83-14 was a gift from K. Siddle (Addenbrooke's Hospital, University of Cambridge, Cambridge, UK), anti-BiP, recombinant hamster BiP, and anti-Cnx were from Stressgen Biotechnologies Corp. (Victoria, British Columbia, Canada), anti-Crt was from Affinity Bioreagents (Golden, CO), and anti-insulin receptor β subunit and antiphosphotyrosine antibodies were from Upstate Biotechnology Inc. (Lake Placid, NY). [^{35}S]Cysteine and [^{35}S]methionine (sp act of >1000 Ci/mmol) were from Amersham Pharmacia Biotech., Inc.

Cell Lines

Stable cell lines expressing the insulin receptor were prepared as described previously using CHO cells (Yoshimasa et al., 1990; Bass et al., 1996). Cells were grown in mininmum essential (MEM) alpha medium containing 10% heat-inactivated dialyzed fetal calf serum, 1 μM methotrexate, 100 U/ml penicillin, and 100 μg/ml streptomycin at 37°C in 5% CO_2.

Metabolic Labeling and Cross-linking

Cell labeling was performed after ~1 h of preincubation in methionine- and cysteine-free DME containing 0.1% bovine serum albumin, 100 U/ml penicillin, and 100 μg/ml streptomycin. Labeling was then performed by the addition of methionine/cysteine-free medium containing 75–100 μCi/ml of [^{35}S]cysteine and [^{35}S]methionine (Amersham Pharmacia Biotech., Inc.; 1,000 Ci/mmol). After labeling for the times indicated in the figure legends, medium was removed and then cells were washed once in PBS or 130 mM NaCl, 20 mM bicine, pH 8.0, on ice. Cell monolayers were lysed in either Triton X-100 lysis buffer (1% Triton X-100, 50 mM Tris-HCl, pH 8.0, 500 mM NaCl, 1 mM $CaCl_2$), or in gentle detergent buffers containing either digitonin (50 mM bicine, pH 8.0, 40 mM NaCl, 5 mM KCl, 10 mM Na_2MoO_4, 0.2% digitonin) or 2% CHAPS, 200 mM NaCl, and 50 mM Hepes. A protease cocktail containing 10 μM PMSF, 5 μg/ml pepstatin, 50 μg/ml leupeptin, and 5 μg/ml aprotinin was included with each lysis buffer. The alkylating agent *N*-ethylmaleimide was added to a final concentration of 5 mM to each lysis buffer when samples were analyzed for oxidative folding intermediates. Where indicated, cross-linking was conducted during lysis with or without 100 μg/ml DSP dithio*bis* (succinimidyl propionate) (Pierce Chemical Co.) on ice for 15–30 min. Cross-linker was inactivated with 10 mM glycine for 10 min on ice, nuclei were pelleted at 14,000 rpm in a bench top microfuge (5415C; Eppendorf Scientific, Inc., Hamburg, Germany), and then the soluble lysate fraction was processed for immunoprecipitation. For pulse-chase analysis, cells were labeled for 15–30 min, washed in PBS, and then chased with 2 mM of L-cysteine and L-methionine for the indicated times. CST was used at a final concentration of 1 mM (prepared by dissolving 5 mg with 65 μl 1N HCl in a final volume of 265 μl to yield 100 mM). TCA precipitation did not reveal significant differences in the amount of protein synthesized between the CST-treated and control groups.

For tryptic destruction of cell surface receptors, at the designated time of chase plates were washed once with PBS and then L-1-tosylamido-2-phenylethyl chloromethyl ketone Trypsin (Pierce Chemical Co.) was added to a final concentration of 0.5 mg/ml in PBS. The plates were agitated at room temperature for 10 min, the trypsin was aspirated on ice, and then the cells were rinsed twice with 1.5 mg/ml of trypsin inhibitor (Boehringer Mannheim Biochemicals) in PBS. The floating cells were pelleted in a microfuge (5415C; Eppendorf Scientific, Inc.) and then combined with cell extracts prepared by scraping the corresponding plates on ice into Triton lysis buffer containing aprotinin.

Immunoprecipitation, Gel Electrophoresis, and Immunoblotting

When immunoprecipitation was performed for analysis of receptor–chaperone complexes, the cell lysates were first precleared by incubation with 5 μl of nonimmune rabbit serum and ~50 μl of protein A for 1 h or more, microfuged, and then transferred to a new tube. Primary immunoprecipitation was performed with an amount of each antibody determined to yield quantitative precipitation. The lysate was combined with protein A–agarose and then adjusted to a final volume of 600 μl with TNNB (50

mM Tris-HCl, pH 8.0, 250 mM NaCl, 0.5% NP-40, 0.5 mM PMSF, 0.1% BSA, and 0.02% NaN_3) before mixing overnight at 4°C. Immune complexes were recovered by brief centrifugation in a bench top microfuge (MF6A; Eppendorf Scienfic, Inc.) and then washed in TNNB, TNNB without BSA (TNN), and finally in PBS before elution in 0.2 M glycine-HCl, pH 2.5. The pH of eluted complexes was neutralized with Tris-HCl, pH 8, and then diluted in concentrated Laemmli sample buffer to yield a final 1× concentration (50 mM Tris-HCl, pH 6.8, 2% SDS, 0.1% bromophenol blue, 10% glycerol, and either 100 mM DDT or 5% β-mercaptoethanol where indicated). Redissolved samples were warmed at 50°C or boiled in reducing agents for 5 min before electrophoresis through 5% stacking and 8% running (5/8%) or 3–10% linear gradient SDS-PAGE at 50–70 V for 18–20 h. After electrophoresis, gels were fixed in a solution of 10% acetic acid and 25% isopropanol and then treated with Amplify. For determination of relative molecular mass, 3–10% gels were stained with Coomassie brilliant blue dye (0.025% Coomassie brilliant blue R-250, 45% methanol, and 9.2% acetic acid) and destained in 7.5% acetic acid and 5% methanol. Gels were dried, exposed to XOMAT film (Eastman Kodak Co., Rochester, NY), and then the fluorograms were analyzed by phosphorimaging the dried gels (model 425E scanner and ImageQuant software, Molecular Dynamics, Inc., Sunnyvale, CA).

Immunoblotting was performed after electrophoresis by transferring the proteins from SDS-PAGE to Immobilon P (membrane presoaked for ~1 min in methanol; Millipore Corp., Waters Chromatography, Milford, MA), in buffer containing 25 mM Tris-HCl, pH 7.4, 192 mM glycine, and 20% methanol at 4°C and 14 V for 12–48 h. The membranes were soaked in blocking buffer (5% wt/vol nonfat dry milk and 0.2% Tween 20 vol/vol in PBS), rinsed in 0.2% Tween 20/PBS three times for 10 min each, and then incubated overnight at 4°C with the primary antibody (or at room temperature for 1 h) while mixing (Scopsi et al., 1995). The membranes were rinsed again in 0.2% Tween 20/PBS, incubated with HRP-linked protein A for 2 h, and then rinsed and developed using ECL reagents (Amersham Pharmacia Biotech. Inc.).

Glycosidase Digestion

After immunoprecipitation, samples were eluted in 50 mM sodium citrate, pH 3.5, and then the pH of the eluates was adjusted to 5.5 (by adding 8 μl of 1.5 M unbuffered sodium citrate to each 150 μl of eluate). Samples digested with endo H (Boehringer Mannheim Biochemicals) were first diluted 1:2 with water, adjusted to ~0.1% SDS, and then heated at 95°C for 5 min. After cooling, PMSF was added to a final concentration of 1 mM, endo H was added to give 30 mU/ml, and then the reaction was incubated at 37°C overnight. The digestion was terminated by boiling in Laemmli sample buffer. Samples digested with neuraminidase were adjusted, pH 5, with 1.5 M sodium acetate, pH 5.5, and then diluted in H_2O to give a final concentration of 50 mM sodium acetate. Calcium chloride was added to a final concentration of 9 mM and *Vibrio cholera* neuraminidase (Calbiochem-Novabiochem Corp., La Jolla, CA) was added to a final concentration of 20 mU/100 μl; because PMSF inhibits neuraminidase, we did not add it to these reaction mixtures. Neuraminidase incubation was at 37°C for 2 h.

Biotinylation

To compare receptor expression levels in control and CST-treated cells, confluent monolayers of CHO cells overexpressing the wild-type receptor were incubated at 37°C for 72 h with CST, washed in Hank's balanced salt solution, and then incubated with 1 mg/ml of sulfo-*N*-hydroxysulfosuccinimide ester-biotin (#21217; Pierce Chemical Co.) for 30 min on ice. Monolayers were washed in PBS containing 15 mM glycine and then lysed in Triton X-100 lysis buffer. Receptors were immunoprecipitated, electrophoresed through 5/8% SDS-PAGE, and then transferred to Immobilon membranes (Millipore Corp.) for blotting with streptavidin-HRP (1:750 dilution; Amersham Pharmacia Biotech. Inc.). ECL was used to visualize the biotinylated receptors and then bands were quantitated by densitometry (Molecular Dynamics, Inc.). Blots were subsequently stripped and reprobed with anti-HIR β subunit antibodies (Upstate Biotechnology Inc., Lake Placid, NY).

Tyrosine Phosphorylation

CHO cells were incubated with cysteine/methionine-free DME containing 75–100 μCi/ml of [^{35}S]methionine and [^{35}S]cysteine for 3–6 h. Cells were then stimulated with the indicated concentrations of insulin at 37°C for 5 min, placed on ice, and then lysed in Triton X-100 lysis buffer containing phosphatase inhibitors (100 mM NaF, 2 mM sodium orthovanadate, 4 mM sodium pyrophosphate). The phosphorylated receptors were recovered by immunoprecipitation with antiphosphotyrosine antibody (6G9) and processed for SDS-PAGE, fluorography, and phosphorimaging. The Student's *t* test was used to determine the significance of differences in receptor autophosphorylation in control and CST-treated cells (Runyon, 1985).

Results

Insulin Receptor Structure and the Identification of the Molecular Basis for Conversion between Four Maturation Intermediates

Fig. 1 shows a linear representation of the extended insulin receptor polypeptide and the structure of the receptor in the cell membrane. The receptor is initially synthesized as a single chain proreceptor that undergoes N-linked glycosylation at 17 consensus sites (Ebina et al., 1985; Ullrich et al., 1985). Before export from the ER, two proreceptor monomers dimerize and form two symmetric interchain covalent disulfide bonds (cysteines 524–524 and 682–682) (Lu and Guidotti, 1996). After maturation of N-linked oligosaccharides and proreceptor proteolytic cleavage by furin or related convertases, as shown by Fuller and Moehring and co-workers (Robertson et al., 1993; Bravo et al., 1994), the receptor is transferred to the plasma membrane as a heterotetramer composed of two α and two β subunits with a molecular mass of 350–400 kD (Olson et al., 1988).

To monitor insulin receptor folding and transport we performed pulse-chase experiments in CHO cell lines

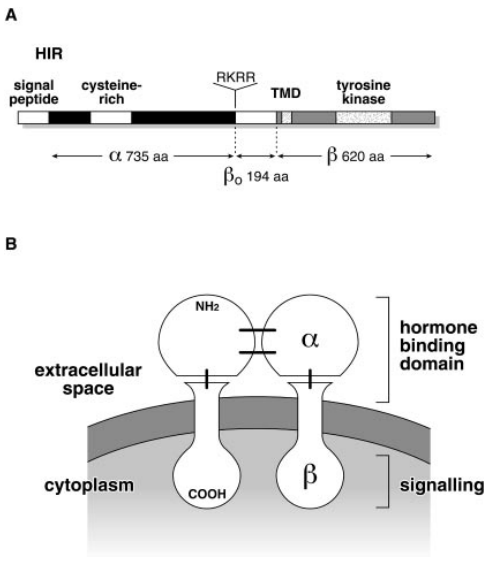

Figure 1. Schematic of insulin receptor structure. (*A*) A linear representation of the insulin receptor precursor protein is shown with functionally important regions highlighted. The proreceptor undergoes N-linked glycosylation at 17 sites and cleavage at the indicated tetrabasic site. (*B*) The mature cell surface insulin receptor is composed of two α and two β subunits that are organized into two separate modules: an extracellular domain consisting of the entire α and part of the β subunits, and an intracellular domain that contains the tyrosine kinase region of the β subunit. The two α subunits are joined by two symmetric interchain disulfide bonds, indicated with dark lines (cysteines 524–524 and 682–682). The plasma membrane heterotetramer has a molecular mass of 350–400 kD.

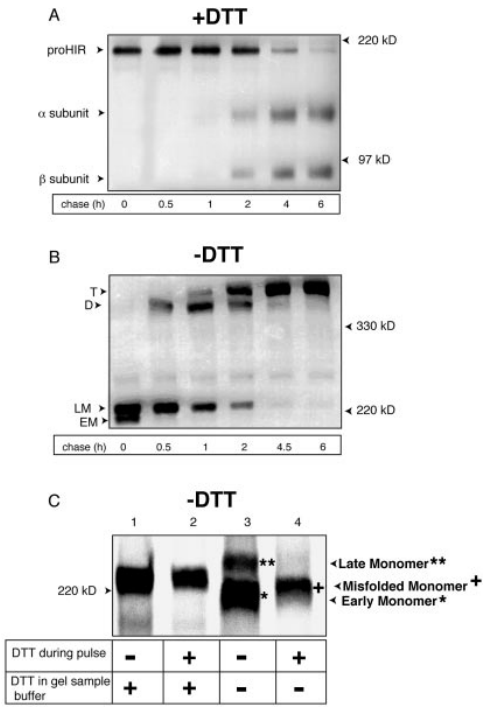

Figure 2. Biosynthesis of the wild-type insulin receptor. (*A*) Stable CHO cells expressing the wild-type insulin receptor were pulse labeled for 30 min with [^{35}S]methionine and [^{35}S]cysteine (50 μCi/ml), washed with PBS, and then chased in medium containing 2 mM each of methionine and cysteine. Cell extracts were prepared at the indicated times, immunoprecipitated, redissolved in Laemmli sample buffer containing DTT, and then electrophoresed through 5/8% SDS-PAGE. The positions of the receptor subunits are indicated with arrows to the left, and two of the molecular weight markers are indicated with arrows to the right (*EM*, early monomer; *LM*, late monomer; *D*, dimer; *T*, tetramer). (*B*) Cells were pulse labeled for 35 min, chased, and then processed under nonreducing conditions by 3–10% linear gradient SDS-PAGE. The position of receptor complexes are indicated with arrows to the left and molecular mass markers are indicated to the right. (*C*) CHO cells were pulse-labeled with [^{35}S]methionine and [^{35}S]cysteine for 15 min in the presence (lanes *2* and *4*) or absence (lanes *1* and *3*) of 5 mM DTT. Cell extracts were immunoprecipitated with anti-HIR antibodies, redissolved in Laemmli sample buffer with (lanes *1* and *2*) and without 10 mM DTT (lanes *3* and *4*) and then analyzed by nonreducing 3–10% SDS-PAGE.

transfected with full-length wild-type receptors (Figs. 1 and 2). Gel electrophoresis was performed under both reducing and nonreducing conditions to follow HIR maturation. After a 30-min pulse, two species were seen, migrating at ~200 and ~220 kD, respectively. With shorter pulse times, the faster migrating band (Fig. 2, *early monomer*, *EM*) appeared first, with radioactivity progressively chasing into the second slower migrating band (Fig. 2, *late monomer*, *LM*).

To determine whether these species represented distinct oxidative intermediates, we followed receptor biosynthesis when the redox environment of the ER was manipulated with the membrane-permeant reducing agent DTT. When the pulse was performed in the presence of 5 mM DTT, the first monomer band to appear migrated to a position slightly above that of the early monomer in untreated cells (Fig. 2 *C*, lane *4*). This intermediate form of the monomeric receptor, which we term "misfolded monomer" (Fig. 2 *C*, lane *4*), failed to progress to a second slower-migrating electrophoretic species. When receptor monomers from both DTT-treated and untreated cells were heated in Laemmli gel buffer with reducing agent before electrophoresis, both migrated to the same position (Fig. 2 *C*, compare lanes *1* and *2* with lane *3*). The fully reduced monomer (Fig. 2 *C*, lanes *1* and *2*) migrated slightly slower than the nonreduced monomer on the same gel (Fig. 2 *C*, lane *3*). Since both the early and late monomers appeared as a single band after reduction (Fig. 2 *C*, lane *1*), we conclude that they differ only in the number and/or arrangement of intramolecular disulfide bonds. Taken together, this suggests that disulfide bond formation occurs rapidly and that the early and late monomers represent two distinct oxidative intermediates of the proreceptor.

After 60 min of chase, a third band of twice the molecular mass (~380 kD) was observed by nonreducing gel electrophoresis. Shortly thereafter, a fourth species appeared (~420 kD), concomitant with movement of the receptor from ER to *trans*-Golgi (Olson et al., 1988). The 380-kD band material was sensitive to digestion with endo H, consistent with its localization in a pre–*trans*-Golgi compartment (data not shown). Acquisition of both endo H resistance and neuraminidase sensitivity coincided with the appearance of the 420-kD species (Fig. 3 *A*), suggesting that this was the mature form of the receptor in the most distal compartment of the secretory pathway.

According to a previous model of insulin receptor biosynthesis proposed by Olson and Lane (1987), the mobility changes described above were ascribed to cleavage of the proreceptor dimer into α and β subunits, possibly reflecting tertiary structural changes associated with proteolytic processing (D to T transition; Olson et al., 1988). To examine whether proteolytic cleavage causes these changes in mobility, we studied the biosynthesis of the R732A mutant proreceptor, which is not cleaved. Such a mutant insulin receptor gene was previously identified in a patient with insulin-resistant diabetes (Yoshimasa et al., 1988, 1990). Surprisingly, despite the lack of proteolytic processing of the R732A proreceptor, the mutant still underwent the same mobility shifts (Fig. 3 *C*). These results suggest that late changes in the electrophoretic mobility of the receptor are due to processing of carbohydrate chains, reflecting movement of the receptor into the *trans*-Golgi (Kornfeld and Kornfeld, 1985), rather than proteolytic cleavage.

Conversion between Early and Late Monomers Involves Interaction with ER Lectin Chaperones Cnx and Crt

To determine whether subunit maturation is facilitated by ER molecular chaperones, we next sought to identify chaperone molecules that associate with newly synthesized receptors. Detergent lysis and chemical cross-linking conditions were optimized to retain associations between newly synthesized receptors and ER resident chaperones. After metabolic labeling and immunoprecipitation with antireceptor antibodies, several coprecipitating proteins were found (Fig. 4 *A*). In addition to the major bands representing the proreceptor and the α and β subunits, two

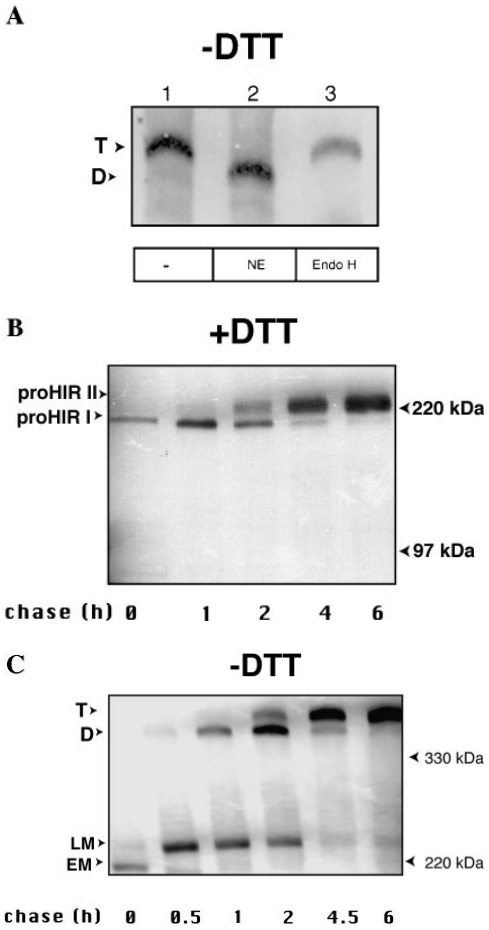

Figure 3. Intracellular movement of the receptor based on endoglycosidase sensitivity and gel shifts. (*A*) CHO cells expressing wild-type receptors were pulse labeled for 30 min and then extracts were prepared after 6 h of chase. Immunoprecipitated receptors were eluted from protein A–agarose in 50 mM sodium citrate, pH 3.5, and incubated with buffer alone (lane *1*), neuraminidase (*NE*, lane *2*), or endo H (*Endo H*, lane *3*). The position of receptor complexes are shown with arrows to the left (*D*, dimer; *T*, tetramer). (*B*) Pulse-chase labeling was performed with CHO cells expressing uncleaved mutant proreceptors containing a substitution in the tetrabasic cleavage site (Arg732Ala). Cells were pulse labeled for 30 min, chased, and then analyzed under reducing conditions by 5/8% SDS-PAGE (proHIR I, first proreceptor with high-mannose oligosaccharides; proHIR II, second proreceptor species containing complex oligosaccharides added in the Golgi). (*C*) CHO cells expressing the R732A mutant receptors were pulse labeled for 15 min, chased, and then analyzed by nonreducing 3–10% linear gradient SDS-PAGE. Folding intermediates and receptor subunits are indicated with arrows to the left and molecular weight markers are indicated to the right (*EM*, early monomer; *LM*, late monomer; *D*, proHIR I dimer; *T*, dimer species after addition of complex oligosaccharides, for simplicity this is labeled using the same nomenclature as that of the wild-type receptor, i.e., the tetramer).

bands were observed migrating faster than the position of the 97-kD β subunit, at ~80 and 90 kD (Fig. 4 *A*, lanes *3* and *4*). These bands were identified as BiP and Cnx, respectively, using specific antibodies (Fig. 4 *A*, lanes *2–4*). No other major bands were reproducibly found.

Three criteria were used to establish that the ~80-kD band was BiP. First, sequential immunoprecipitation with antireceptor antibodies followed by immunoblotting with anti-BiP antibodies, showed BiP immunoreactivity of the ~80-kD band (Fig. 4 *B*). Second, the ~80-kD band comigrated with recombinant hamster BiP as demonstrated by silver staining the gels (data not shown). Finally, cell lysis in the presence of 10 mM ATP dissociated BiP–receptor complexes (Fig. 4 *A*, compare lane *7* with lane *10*). Complexes between HIR and BiP were most stable when lysis was performed in the presence of the cross-linking agent DSP (see Fig. 11 *C*, lanes *4* and *5*), although ATP-sensitive association with BiP was also detectable by Western blot in the absence of cross-linking agent (Fig. 4 *B*, lanes *2* and *3*). We found that the anti-BiP antibody reacted only poorly in immunoprecipitation reactions explaining the consistently lower amount of HIR recovered in anti-BiP precipitates (Fig. 4). However, this antibody, which was raised to a synthetic COOH-terminal peptide, reacted well by immunoblotting (Stressgen anti-Grp 78; Fig. 4 *B*).

The identity of the ~90-kD band was confirmed by coimmunoprecipitation with anti-Cnx antibodies that coprecipitated both Cnx and the insulin proreceptor. The observation that anti-Cnx antibodies selectively coprecipitated the proreceptor and not the cleaved α or β subunits is consistent with an association between calnexin and the receptor in the early secretory pathway before cleavage into these subunits (Fig. 4 *A*, compare lanes *3* and *4*). Furthermore, inhibition of glucose trimming by preincubating cells with CST before lysis, a manipulation that has been shown to disrupt the carbohydrate binding site for Cnx, led to dissociation of Cnx–proreceptor complexes (Fig. 5 *A*). Similarly, complexes between the insulin receptor and Crt, a second ER lectin chaperone, were also demonstrated by coimmunoprecipitation with anti-Crt antibodies (Fig. 5 *B*). Although it is possible that CST effects an intermediate glycoprotein or another ER chaperone required for Cnx/Crt–HIR binding, it is clear that Cnx/Crt–HIR complexes were dissociated after CST treatment. Proreceptors isolated from cells treated with CST migrated more slowly on SDS-PAGE, consistent with the presence of additional glucose moieties attached to the 17 N-linked carbohydrate side chains present in the ectodomain; this also provided an independent confirmation that CST was effective in blocking glucose trimming (Fig. 5, *A* and *B*, *αHIR*). Together, the results suggest that the coprecipitation of the proreceptor by anti-Cnx antibodies is due to specific chaperone–receptor interactions.

To identify whether Cnx and Crt associate with both the monomeric and dimeric receptors, or only a subset of receptors, Cnx–HIR complexes were analyzed by nonreducing SDS-PAGE. Because of variable recovery with different bleeds of the Cnx and Crt immune serum, and because both antibodies precipitated less proHIR than antireceptor antibodies, we used more total cell lysate for immunoprecipitation with Cnx/Crt antibodies than HIR antibodies. Furthermore, we found that the anti-Crt antibody consistently recovered more HIR than comparable amounts of anti-Cnx antibodies (Fig. 5 *C*, lanes *3* and *4*). The relatively greater quantitative yields with the anti-Crt versus anti-Cnx antibodies have also been observed in fibroblast cultures (Green, W.N., personal communication). An additional high molecular weight band that was present after

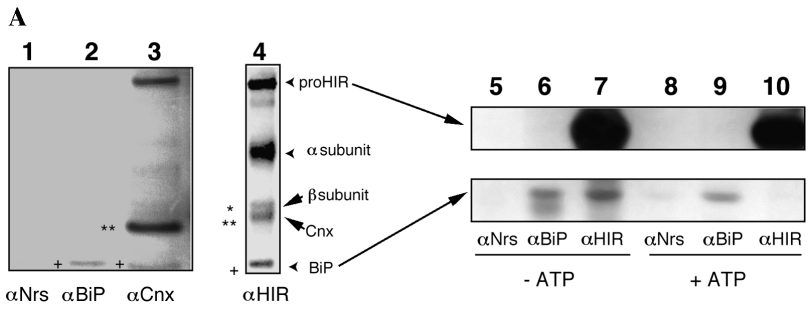

Figure 4. Isolation of ternary BiP–Cnx–HIR complexes. (*A*) CHO cells overexpressing wild-type receptors were labeled overnight with [^{35}S]methionine and [^{35}S]cysteine 50 μCi/ml and then lysed in 0.4% digitonin with DSP. Samples in lanes *1–3* were from the same experiment, and the lysate was divided equally, immunoprecipitated, and then processed for 5/8% SDS-PAGE (lane *1*, αNRS [normal rabbit serum]; lane *2*, αBiP; lane *3*, αCnx; lane *4*, αHIR). The positions of BiP (+), Cnx (**), and the β subunit (*) are indicated to the left in lanes *2–4.* A separate analysis from another experiment is shown in lane *4* to more clearly delineate the receptor and chaperone bands; a similar pattern was obtained by immunoprecipitation of the sample shown in lanes *1–3.* The positions of receptor subunits, Cnx and BiP are indicated with arrows. (*Lanes 5–10*) Cells were labeled as in lanes *1–4*, and lysis was performed without (lanes *5–7*) or with (lanes *8–10*) 10 mM ATP. (*B*) Equivalent amounts of cell lysate protein from CHO cell lines were immunoprecipitated with anti-HIR antibodies, electrophoresed under reducing conditions through 5/8% SDS-PAGE, transferred to immobilon membranes, immunoblotted with anti-BiP antibody, and then developed with ECL reagents (lane *1*, recombinant BiP; lanes *2* and *3*, cells expressing wild-type receptors) (Bass et al., 1996).

precipitation with anti-Crt antibodies appeared to migrate close to the position of the dimeric receptor species; however, this band was not precipitated with antireceptor antibodies (Fig. 5 *C*, lanes *2* and *4*). Additional experiments performed at later chase times failed to show association between dimeric receptors and Cnx/Crt, and recent sucrose gradient analysis confirms that association of Cnx is restricted to monomeric forms of the receptor (data not shown). Since dimeric receptors typically convert to the tetramer after a brief lag period, it is likely that release from Cnx/Crt occurs before dimerization and export from the ER (refer to Fig. 2).

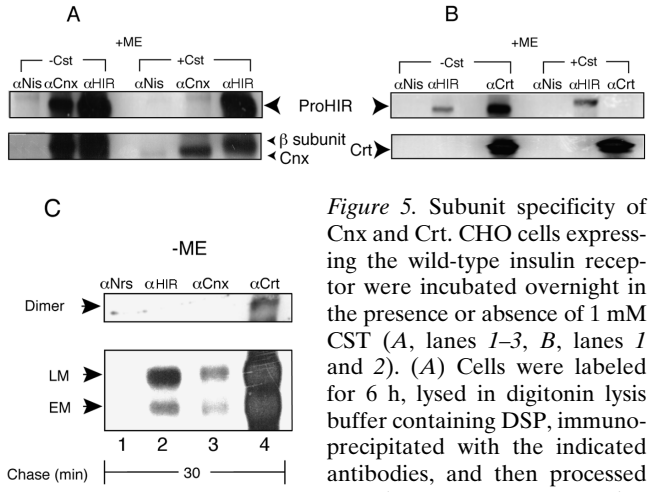

Figure 5. Subunit specificity of Cnx and Crt. CHO cells expressing the wild-type insulin receptor were incubated overnight in the presence or absence of 1 mM CST (*A*, lanes *1–3*, *B*, lanes *1* and *2*). (*A*) Cells were labeled for 6 h, lysed in digitonin lysis buffer containing DSP, immunoprecipitated with the indicated antibodies, and then processed for 5/8% SDS-PAGE using β-mercaptoethanol as the reducing agent (*ME*). (*B*) Cells were labeled for 5 h, lysed in CHAPS lysis buffer without cross-linking, and then processed for 5/8% SDS-PAGE as in *A*. The positions of the proreceptor, Cnx, and Crt are indicated with arrows to the left. Note that the receptor β subunit has a molecular mass of ~95 kD and migrates close to the position of Cnx, which has a molecular mass of ~90 kD (*A*, lanes *3* and *6*). (*C*) Cells were pulse labeled for 30 min and then lysed in digitonin buffer after a 30-min chase (lanes *1–4*). Equivalent aliquots of lysate were processed for immunoprecipitation with nonimmune serum (lanes *1* and *4*), anti-Cnx (lane *3*), and anti-Crt (lane *4*), and one-third of this amount was processed for immunoprecipitation with anti-HIR (lane *2*). Immunoprecipitated protein was analyzed under nonreducing conditions by 3–10% SDS-PAGE. The positions of the early monomer (*EM*), late monomer (*LM*), and dimer are indicated with arrows.

Delayed ER Export and Accelerated Dimerization Occur When Binding to Lectin Chaperones Is Blocked

To analyze the effects of Cnx and Crt on receptor maturation, we performed pulse-chase studies after incubation with CST. In CST-treated cells, there was a consistent delay in the processing of the proreceptor into α and β subunits at late chase time points (Fig. 6). However, no significant difference in recovery of total ^{35}S-labeled receptor was detected at time points up to 7 h of chase, suggesting that the delay in cleavage did not result in accelerated receptor degradation at these time points (data not shown). Since proteolytic cleavage of the proreceptor has been localized to the *trans*-Golgi apparatus (Molloy et al., 1994), unprocessed proreceptors must have accumulated in a pre-TGN compartment after CST treatment. The half-life of the total processed (α and β subunits) and unprocessed proreceptor in both CST-treated and untreated groups was ~10 h (Fig. 6). These values are in agreement with previous measurements by both Kahn and Lane and coworkers (Kasuga et al., 1981; Ronnett et al., 1983). Although these results suggest that the overall turnover rate of proHIR, α and β subunits was unchanged after CST treatment, it is possible that unprocessed proreceptors in CST-treated cells are retained in the ER and degraded rather than transported to the cell surface.

The lack of binding to lectin chaperones after CST treatment suggested that retention of the dimeric pool of receptors in the treated group occurred through a calnexin-independent mechanism. To examine whether the retained receptors in CST-treated cells were associated more avidly with BiP, we performed immunoblotting with anti-BiP antibodies after immunoprecipitation with anti-HIR antibodies. Fig. 7 shows two- to threefold increases in the amount of BiP associated with the receptor in CST-treated compared to control cells. This suggests that BiP is

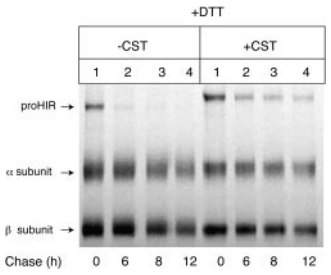

Figure 6. Receptor turnover in CST-treated and untreated cells. CHO cells were treated with CST or in labeling medium alone in the presence of [^{35}S]methionine and [^{35}S]cysteine. The plates were then washed and chased in medium containing excess methionine and cysteine. Cell extracts were prepared at the indicated times in Triton X-100 lysis buffer, immunoprecipitated with αHIR antibodies, redissolved in Laemmli sample buffer containing DTT, and then electrophoresed through 5/8% SDS-PAGE. A fluorogram from a representative experiment is shown. Receptor subunits are indicated with arrows to the left.

involved in retaining proreceptor molecules, which accumulate after blockade of binding to the lectin chaperones.

Surprisingly, analysis of receptor biosynthesis after CST treatment on nonreducing gels showed that conversion from the early monomer to the late monomer and dimerization were all greatly accelerated after CST treatment (Fig. 8 *A*). Accelerated formation of early and late monomers is more clearly observed in the fluorogram shown in Fig. 8 *B*. However, it is possible that the early and late monomers detected after CST treatment have subtle structural abnormalities compared to wild-type receptors; such structural differences might not be detected on SDS-PAGE analysis. The increased rate of receptor dimerization in CST-treated cells is clearly noted when the phosphorimaging data from two separate pulse-chase experiments was represented by a histogram (Fig. 8 *D*). Earlier dimerization in CST-treated cells was reproducibly found in five additional experiments performed with varied pulse times (data not shown). To test whether dimeric receptors produced in the presence of CST progressed more rapidly to the cell surface, we incubated cells at varying time points with trypsin, which specifically releases only the cell surface receptors (Shoelson et al., 1988). Transport of these receptors to the cell surface was demonstrated by the trypsin sensitivity of receptors from treated and untreated cells (Fig. 8 *C*). Moreover, trypsin-sensitive receptors were

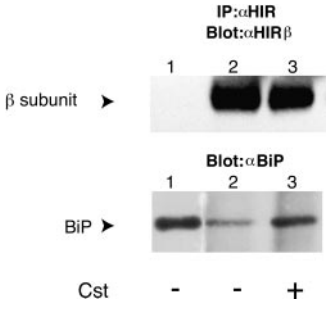

Figure 7. Effect of CST treatment on BiP–HIR association. CST-treated and control CHO cells expressing the wild-type receptor were prepared as described in Fig. 6 except lysis was performed in CHAPS buffer. Cell lysate protein was measured using the Bio-Rad DC protein reagent and equivalent amounts of lysate protein were immunoprecipitated with anti-HIR antibodies, followed by reducing gel electrophoresis and immunoblotting with anti-HIR (*top*) and anti-BiP (*bottom*) antibodies. Samples shown in both upper and lower panels are as follows: 5 μg of recombinant BiP (lane *1*), anti-HIR immunoprecipitated lysate from control cells (lane *2*), and from CST-treated cells (lane *3*).

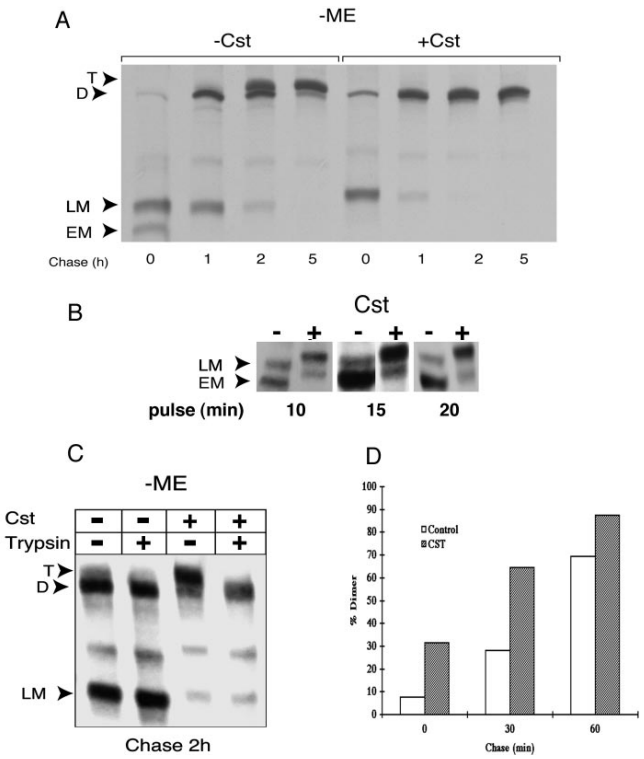

Figure 8. Kinetics of proreceptor folding after CST treatment. (*A*) Cells were pulse-labeled for 30 min in [^{35}S]methionine and [^{35}S]cysteine (100 μCi/ml) and then chased for the indicated times. The positions of the intermediates are indicated with arrowheads (*EM*, early monomer; *LM*, late monomer; *D*, dimer; *T*, tetramer). The conversion from dimer to tetramer species in CST-treated cells was obscured due to the higher molecular weight associated with excess untrimmed glucose residues attached to the Asn-linked saccharide chains. Samples were analyzed under nonreducing conditions on 3–10% linear gradient SDS-PAGE. (*B*) Cst-treated and control cells were pulse labeled for various times and then analyzed as in *A*. *EM* and *LM*, the only species present in untreated cells at these early time points, are indicated with arrows. (*C*) Cst-treated and control cells were pulse labeled for 20 min, chased for 2 h, and then incubated for 10 min at 25°C in the presence of trypsin (0.5 mg/ml) to release cell-surface receptors before processing as described for Fig. 2. The highest molecular mass species (*T*) in both Cst-treated and control groups was trypsin sensitive, whereas the lower molecular mass species (*D*) remained trypsin resistant. (*D*) Histogram representing the rate of dimerization of receptors in Cst-treated versus control cells. Phosphorimaging data from two experiments with 30-min pulse times was compiled and expressed as the percentage of total radioactivity present at each time point as the dimer.

found at earlier times in CST-treated cells, and proteolytic cleavage of a subset of proreceptors into α and β subunits was similarly detected at an earlier time point (comparing α and β subunits visible at a 1 h time point in CST-treated versus untreated cells, data not shown). Based on insulin cross-linking studies, we found that all of the receptors present on the cell surface were, in fact, processed into α and β subunits since insulin was only detected bound to the α subunit and not to the proreceptor (data not shown). However, despite the rapid dimerization and transport to the cell surface of a subset of newly synthesized receptors,

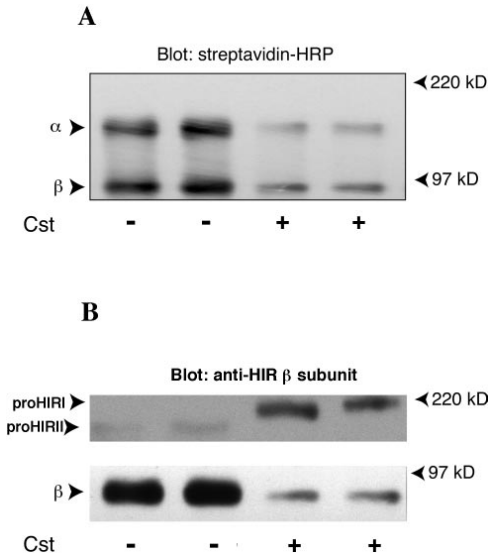

Figure 9. Biotinylation of cells treated with Cst. (*A*) Cell surface receptors were biotinylated after a 72-h incubation with Cst. Cells were solubilized in Triton lysis buffer and then processed for immunoprecipitation with anti-HIR antibodies and analysis by reducing 5/8% SDS-PAGE. Biotinylation was detected after transfer of the proteins to Immobilon P using streptavidin–HRP and ECL (Amersham Pharmacia Biotech. Inc.). (*B*) Blots were stripped and reprobed with anti-HIR β subunit antibodies. Receptor subunits and the position of molecular weight markers are indicated with arrows.

a fraction of the dimeric pool of receptors remained uncleaved and were retained in a pre-TGN compartment (Fig. 6).

Functional Receptors Are Delivered to the Cell Surface in CST-treated Cells

To assess levels and function of cell surface receptors in CST-treated and control cells, both biotinylation and insulin-stimulated tyrosine autophosphorylation were used. Fig. 9 *A* shows that cell surface biotinylation of receptors was decreased (~30% when three separate experiments were compared) in CST-treated cells, whereas steady-state levels of the proreceptor were increased (Fig. 9 *B*). Total cellular levels of processed β subunit were also decreased at steady state (Fig. 9 *B*). The decreased level of the β subunit is consistent with the retention and/or degradation of CST-treated receptors in an unprocessed form in the early secretory pathway.

To measure the ability of the bound hormone to transmit a signal to the intracellular domain of the receptor, we compared insulin-stimulated tyrosine phosphorylation of the receptor in CST-treated and control groups. Fig. 10 shows that insulin-responsive autophosphorylation, measured by recovery of prelabeled receptor protein after brief incubation with insulin, was equivalent in control and CST-treated groups. Together, the results show that steady-state levels of processed and cell surface receptors were decreased after CST treatment, although receptors delivered to the cell surface were fully responsive to hormone. The correct folding of a majority of receptors in the presence of CST suggests that lectin-based interactions are not essential; rather, they enhance or facilitate folding.

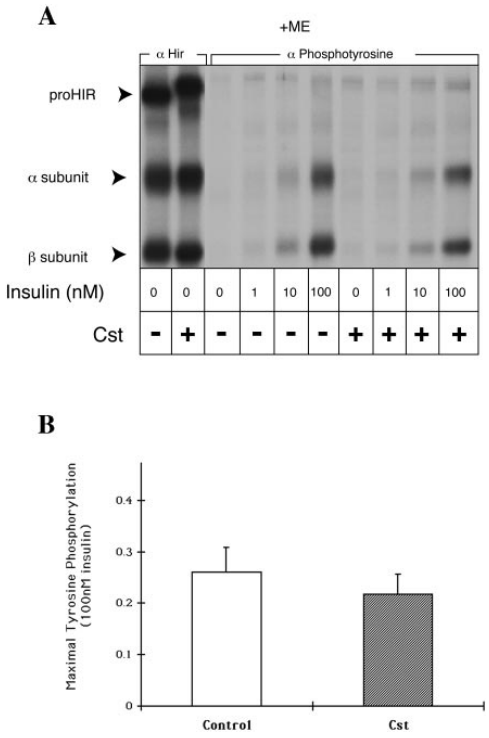

Figure 10. Insulin-induced receptor autophosphorylation in cells treated with CST. (*A*) Cells were incubated overnight in 1 mM CST and labeled with [^{35}S]cysteine and [^{35}S]methionine (75 μCi/ml of each) for 5 h. The cells were then stimulated with insulin for 5 min at 37°C (0–100 nM), washed in PBS, lysed in Triton buffer containing phosphatase inhibitors and equivalent amounts of lysate were processed for immunoprecipitation either with anti-HIR or antiphosphotyrosine antibodies. (*B*) Histogram showing the relative percentage of tyrosine-phosphorylated receptors recovered after stimulation with 100 nM insulin in CST-treated versus control cells. No significant difference was found comparing the two groups (mean ± standard error, $n = 3$; data from three separate experiments).

Discussion

Recently, a number of studies have demonstrated that both lectin chaperones and the Hsp70 homologue BiP mediate the folding and assembly of oligomeric membrane proteins (Hammond and Helenius, 1994*a*,*b*; Williams and Watts, 1995). In vitro studies have shown that CST treatment of canine microsomes accelerates the oligomerization of HA, an exogenous viral protein (Hebert et al., 1996). The present studies establish a new model system to investigate the role of individual chaperone molecules in endogenous membrane protein folding in living cells. This model is based on experiments that define in more detail the molecular basis for individual maturation steps in insulin receptor biosynthesis. The results further provide evidence that N-linked glycosylation, and interaction with Cnx and Crt, delays dimerization and facilitates folding to a transport-competent conformation analogous to the effects with HA (Hebert et al., 1996). Because CST directly affects glucose trimming from N-linked glycans in HIR, it is possible that misfolding is due to disrupted carbohydrate maturation per se. Overall, we found that the integrated effects of N-linked glycosylation and chaperone

binding regulate the production of functional insulin receptors and influences the rate at which individual subunits assemble into homodimers.

The prolonged period that elapses before dimerization exposes the nascent proreceptor to the aqueous oxidizing environment of the ER. However, under normal growth conditions, biosynthesis is highly efficient and more than 90% of newly synthesized receptors were delivered to the cell surface (refer Fig 2). Interaction with Cnx and Crt might provide protection of exposed hydrophobic domains, preventing their misfolding and aggregation. Association with either Cnx or Crt could create steric hindrance, possibly by interacting with a surface that later becomes inaccessible in the dimer. This might provide sufficient time for partially folded forms to undergo refolding and attain their native conformation (Hebert et al., 1996; Vassilakos et al., 1996).

The delayed movement of a subset of proreceptors to the *trans*-Golgi after treatment of cells with CST suggests that these receptors were misfolded (refer to Figs. 6 and 7). ER retention of these dimeric receptors was independent of Cnx and Crt based on coprecipitation assays (refer to Fig. 5). The persistence of BiP–receptor complexes after CST treatment could explain the retention of these receptor dimers. BiP might additionally protect the retained receptors and promote their eventual resolubilization. Since growth factor receptors have been shown to be important for survival of mammalian cells in culture, calnexin-independent production of insulin receptors might account for the continued viability of CST-treated cells (Figs. 9 and 10; Arakaki et al., 1987; Baserga, 1994; Rubini et al., 1997). In addition to BiP, an alternative ER retention mechanism for prematurely dimeric receptors might be the presence of free thiols that flag such molecules and promote their arrest (Isidoro et al., 1996).

Fig. 11 illustrates a model in which two competing reactions exist in a hierarchy during receptor biosynthesis. Under normal growth conditions, the first reaction, in which monomeric receptor halves associate with Cnx and Crt, predominates. This leads to slow but highly efficient production of functional receptors. In the second competing reaction, shown as the lower pathway in Fig. 11, dimerization is much more rapid (<25 min), after blockade of N-linked glycosylation. Rapid dimerization leads to less overall efficient maturation and retention of dimeric or aggregated receptors in the ER. In this default pathway, binding to BiP is preserved, perhaps protecting the retained receptors until they achieve a transport-competent conformation.

In conclusion, these studies have shown that lectin chaperones directly associate with newly synthesized insulin receptors during disulfide bond formation and isomerization, whereas blockade of glucose trimming dissociates Cnx/Crt–HIR complexes and corresponds with accelerated dimerization and delayed maturation. Experiments with CST suggest that folding to a transport-competent conformation requires a posttranslational delay in homodimerization. Two possible mechanisms could account for the effects of Cnx/Crt on receptor folding: (*a*) Cnx/Crt could either simply facilitate folding to a dimerization-competent conformation, or (*b*) they could directly mediate the dimerization reaction. The development of an in vivo system to examine Cnx/Crt and BiP interactions with a membrane protein provides further opportunity to study how these interactions mediate the ER retention of misfolded receptors in cases of diabetes caused by mutations in the receptor gene. Additionally, these interactions might be important during embryogenesis (e.g., insulin growth factor [IGF]-I receptor) or during differentiation from fibroblast to adipocyte (e.g., insulin receptor) when

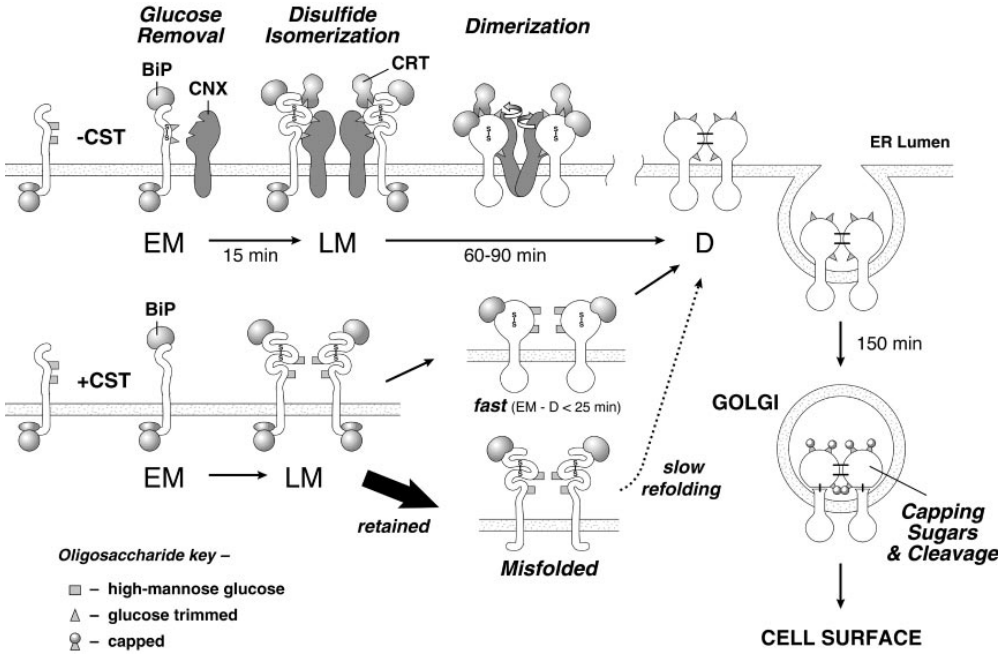

Figure 11. Maturation model. Temporal sequence of ER folding of the insulin receptor showing synchronization of maturation and chaperone binding. The diagram illustrates that Cnx/Crt bind in complexes to newly synthesized proreceptor monomers (*EM*, early monomer) and that conversion to a second oxidative intermediate (*S–S*) occurs during binding to chaperones (*LM*, late monomer). Post-ER maturation involves proteolytic cleavage and addition of carbohydrate capping sugars to Asn-linked oligosaccharide chains. Addition of carbohydrates results in mobility shifts on nonreducing SDS-PAGE, whereas proteolytic cleavage does not alter the tertiary or quaternary structure of the receptor as detected by nonreducing SDS-PAGE. The dual pathways of maturation involve either Cnx/Crt and BiP (*top route*) with dimerization occurring at ~75 min posttranslationally, whereas a second pathway occurs when Cnx/Crt are bypassed with rapid dimerization within ~10 min posttranslationally.

rapid increases in receptor synthesis are required. Studies are in progress with mutant forms of HIR in recombinant cells to further examine the basis of Cnx/Crt association with HIR, to determine the mechanisms of HIR retention and degradation, and to search for possible additional ER proteins that might be involved in this process.

We thank B. Green for helpful discussions, M. Milewski for technical assistance, W. Chutkow for graphics, S. Duguay and B. Glick for comments on the manuscript, and R. Ricks (all six from University of Chicago, Chicago, IL) for assistance in preparation of the manuscript.

This work was supported by the Howard Hughes Medical Institute and in part by National Institutes of Health grants (DK 13914 and DK20595).

Received for publication 10 November 1997 and in revised form 4 March 1998.

References

Arakaki, R.F., J.A. Hedo, E. Collier, and P. Gorden. 1987. Effects of castanospermine and 1-deoxynojirimycin on insulin receptor biogenesis: evidence for a role of glucose removal from core oligosaccharides. *J. Biol. Chem.* 262: 11886–11892.

Aridor, M., and W.E. Balch. 1996. Principles of selective transport: coat complexes hold the key. *Trends Cell Biol.* 6:315–320.

Baserga, R. 1994. Oncogenes and the strategy of growth factors. *Cell.* 79:927–930.

Bass, J., T. Kurose, M. Pashmforoush, and D.F. Steiner. 1996. Fusion of insulin receptor ectodomains to immunoglobulin constant domains reproduces high-affinity insulin binding *in vitro*. *J. Biol. Chem.* 271:19367–19375.

Bergeron, J.J.M., M.B. Brenner, D.Y. Thomas, and D.B. Williams. 1994. Calnexin: a membrane-bound chaperone of the endoplasmic reticulum. *Trends Biochem. Sci.* 19:124–128.

Bravo, D.A., J.B. Gleason, R.I. Sanchez, R.A. Roth, and R.S. Fuller. 1994. Accurate and efficient cleavage of the human insulin proreceptor by the human proprotein-processing protease furin: characterization and kinetic parameters using the purified, secreted soluble protease expressed by a recombinant baculovirus. *J. Biol. Chem.* 269:25830–25837.

Brodsky, J.L., J. Groeckeler, and R. Schekman. 1995. BiP and Sec63P are required for both co- and posttranslational protein translocation into the yeast endoplasmic reticulum. *Proc. Natl. Acad. Sci. USA.* 92:9643–9646.

David, V., F. Hachstenback, S. Rajagopalan, and M.B. Brenner. 1993. Interaction with newly synthesized and retained proteins in the endoplasmic reticulum suggests a chaperone function for human integral membrane protein IP90 (calnexin). *J. Biol. Chem.* 268:9585–9592.

Ebina, Y., L. Ellis, K. Jarnagin, M. Edery, L. Graf, E. Clauser, J.-h. Ou, F. Masiarz, Y.W. Kan, I.D. Goldfine, et al. 1985. The human insulin receptor cDNA: the structural basis for hormone-activated transmembrane signaling. *Cell.* 40:747–758.

Gething, M.-J., and J. Sambrook. 1992. Protein folding in the cell. *Nature.* 355: 33–45.

Hammond, C., and A. Helenius. 1994*a.* Quality control in the secretory pathway: retention of a misfolded viral membrane glycoprotein involves cycling between the ER, intermediate compartment, and Golgi apparatus. *J. Cell Biol.* 126:41–52.

Hammond, C., and A. Helenius. 1994*b.* Folding of VSV G protein: sequential interaction with BiP and calnexin. *Science.* 266:456–458.

Hammond, C., I. Braakman, and A. Helenius. 1994. Role of N-linked oligosaccharide recognition, glucose trimming, and calnexin in glycoprotein folding and quality control. *Proc. Natl. Acad. Sci. USA.* 91:913–917.

Hartl, F.U. 1996. Molecular chaperones in cellular protein folding. *Nature.* 381: 571–580.

Hebert, D.N., B. Foellmer, and A. Helenius. 1995. Glucose trimming and reglucosylation determine glycoprotein association with calnexin in the endoplasmic reticulum. *Cell.* 81:425–433.

Hebert, D.N., B. Foellmer, and A. Helenius. 1996. Calnexin and calreticulin promote folding, delay oligomerization and suppress degradation of influenza hemagglutinin in microsomes. *EMBO (Eur. Mol. Biol. Organ.) J.* 5:2961–2968.

Helenius, A. 1994. How N-linked oligosaccharides affect glycoprotein folding in the endoplasmic reticulum. *Mol. Biol. Cell.* 5:253–266.

Helenius, A, T. Marquardt, and I. Braakman. 1992. The endoplasmic reticulum as a protein-folding compartment. *Trends Cell Biol.* 2:227–231.

Isidoro, C., C. Maggioni, M. Demoz, A. Pizzagalli, A.M. Fra, and R. Sitia. 1996. Exposed thiols confer localization in the endoplasmic reticulum by retention rather than retrieval. *J. Biol. Chem.* 271:26138–26142.

Jackson, M.R., M.F. Cohen-Doyle, P.A. Peterson, and D.B. Williams. 1994. Regulation of MHC class I transport by the molecular chaperone, calnexin (p88, IP90). *Science.* 263:384–386.

Kasuga, M., C.R. Kahn, J.A. Hedo, E. Van Obberghen, and K.M. Yamada. 1981. Insulin-induced receptor loss in cultured human lymphocytes is due to accelerated receptor degradation. *Proc. Natl. Acad. Sci. USA.* 78:6917–6921.

Kornfeld, R., and S. Kornfeld. 1985. Assembly of asparagine-linked oligosaccharides. *Annu. Rev. Biochem.* 54:631–664.

Kozutsumi, Y., M. Segal, K. Normington, M.-J. Gething, and J. Sambrook. 1988. The presence of malfolded proteins in the endoplasmic reticulum signals the induction of glucose-regulated proteins. *Nature.* 332:462–464.

Krause, K., and M. Michalak. 1997. Calreticulin. *Cell.* 88:439–443.

Lodish, H.F. 1986. Transport of secretory and membrane glycoproteins from the rough endoplasmic reticulum to the Golgi: a rate-limiting step in protein maturation and secretion. *J. Biol. Chem.* 263:2107–2110.

Lodish, H.F., and N. Kong. 1984. Glucose removal from N-linked oligosaccharides is required for efficient maturation of certain secretory glycoproteins form the rough endoplasmic reticulum to the Golgi complex. *J. Cell Biol.* 98: 1720–1729.

Loo, T.W., and D.M. Clarke. 1994. Prolonged association of temperature-sensitive mutants of human p-glycoprotein with calnexin during biogenesis. *J. Biol. Chem.* 269:28683–28689.

Lu, K., and G. Guidotti. 1996. Identification of the cysteine residues involved in the class I disulfide bonds of the human insulin receptor: properties of insulin receptor monomers. *Mol. Biol. Cell.* 7:679–691.

Lyman, S.K. and R. Scheckman. 1997. Binding of secretory precursor polypeptides to a translocon subcomplex is regulated by BiP. *Cell.* 88:85–96.

Molloy, S.S., L. Thomas, J.K. VanSlyke, P.E. Stenberg, and G. Thomas. 1994. Intracellular trafficking and activation of the furin proprotein convertase: localization to the TGN and recycling from the cell surface. *EMBO (Eur. Mol. Biol. Organ.) J.* 13:18–33.

Munro, S., and H.R.B. Pelham. 1986. An Hsp70-like protein in the ER: identity with the 78 kd glucose-regulated protein and imunoglobulin heavy chain binding protein. *Cell.* 46:291–300.

Olson, T.S. and M.D. Lane. 1987. Post-translational acquisition of insulin binding activity by the insulin proreceptor: correlation to recognition by autoimmune antibody. *J. Biol. Chem.* 262:6816–6822.

Olson, T.S., M.J. Bamberger, and M.D. Lane. 1988. Post-translational changes in the tertiary and quaternary structure of the insulin proreceptor: correlation with acquisition of function. *J. Biol. Chem.* 263:7342–7351.

Ou, W.-J., P.H. Cameron, D.Y. Thomas, and J.J.M. Bergeron. 1993. Association of folding intermediates of glycoproteins with calnexin during protein maturation. *Nature.* 364:771–776.

Pind, S., J.R. Riordan, and D.B. Williams. 1994. Participation of the endoplasmic reticulum chaperone calnexin (p88, IP90) in the biogenesis of the cystic fibrosis transmembrane conductance regulator. *J. Biol. Chem.* 269:12784–12788.

Robertson, B.J., J.M. Moehring, and T.J. Moehring. 1993. Defective processing of the insulin receptor in an endoprotese-deficient chinese hamster cell strain is corrected by expression of mouse furin. *J. Biol. Chem.* 268:24274–24277.

Ronnett, G.V., G. Tennekoon, V.P. Knutson, and M.D. Lane. 1983. Kinetics of insulin receptor transit to and removal from the plasma membrane: effect of insulin-induced down-regulation in 3T3-L1 adipocytes. *J. Biol. Chem.* 258: 283–290.

Rubini, M., A. Hongo, C. D'Ambrosio, and R. Baserga. 1997. The IGF-I receptor in mitogenesis and transformation of mouse embryo cells: role of receptor number. *Exp. Cell Res.* 230:284–292.

Runyon, R.P. 1985. Fundamentals of Statistics. Duxbury Press, Boston, MA. 393 pp.

Scopsi, L., M. Gullo, F. Rilke, S. Martin, and D.F. Steiner. 1995. Proprotein convertases (PC1/PC3 and PC2) in normal and neoplastic human tissues: their use as marker of neuroendocrine differentiation. *J. Clin. Endocrinol. Metab.* 80:294–391.

Shoelson, S.E., M.F. White, and C.R. Kahn. 1988. Tryptic activation of the insulin receptor: proteolytic truncation of the α-subunit releases the β-subunit from inhibitory control. *J. Biol Chem.* 263:4852–4860.

Ullrich, A., J.R. Bell, E.Y. Chen, R. Herrera, L.M. Petruzzelli, T.J. Dull, A. Gray, L. Coussens, Y.-C. Liao, M. Tsubokawa, et al. 1985. Human insulin receptor and its relationship to the tyrosine kinase family of oncogenes. *Nature.* 313:756–761.

Vassilakos, A., M.F. Cohen-Doyle, P.A. Peterson, M.R. Jackson, and D.B. Williams. 1996. The molecular chaperone calnexin facilitates folding and assembly of class I histocompatibility molecules. *EMBO (Eur. Mol. Biol. Organ.) J.* 15:1495–1506.

Williams, D.B., and T.H. Watts. 1995. Molecular chaperones in antigen presentation. *Curr. Opin. Immunol.* 7:77–84.

Yoshimasa, Y., S. Seino, J. Whittaker, T. Kakehi, A. Kosaki, H. Kuzuya, H. Imura, G.I. Bell, and D.F. Steiner. 1988. Insulin-resistant diabetes due to a point mutation that prevents insulin proreceptor processing. *Science.* 240: 784–787.

Yoshimasa, Y., J.I. Paul, J. Whittaker, and D.F. Steiner. 1990. Effects of amino acid replacements within the tetrabasic cleavage site on the processing of the human insulin receptor precursor expressed in chinese hamster ovary cells. *J. Biol Chem.* 265:17230–17237.

Zapun, A., S.M. Petrescu, P.M. Rudd, R.A. Dwek, D.Y. Thomas, and J.J.M. Bergeron. 1997. Conformation-independent binding of monoglucosylated ribonuclease B to calnexin. *Cell.* 88:29–38.